Assessment of Post-Earthquake Damage in RC Elements Using Low-Invasive Techniques

A. Malek, A. Scott, S. Pampanin & G.A. MacRae

Department of Civil and Natural Resources Engineering, University of Canterbury, Christchurch, New Zealand

2015 NZSEE Conference

ABSTRACT: The crucial need for reliable and practical low-invasive methods to assess the structural conditions, including level of damage and residual capacity, of RC structures after an earthquake has been highlighted in the recent earthquake events. Taking a decision on, whether a damaged structure should be demolished or repaired, directly depends on data and information collected from site investigations.

As a part of a broader research project on residual capacity of RC structures, this study intends to correlate observed damage with material degradation in the concrete. Following an overview of traditional low-invasive techniques used in practice or more recently proposed in literature, the paper presents the outcomes of two alternative approaches based on concrete durability tests as well as image detection method.

In the first phase of the experimental campaign, concrete cylinders were monotonically loaded under uniaxial compression up to certain stress levels. A combination of oxygen permeability, electrical resistivity and porosity tests were employed to quantify damage on disks sawn from one-third middle part of samples. Results showed that permeability test can be useful to assess the damaged concrete as permeability coefficient increases with a great sensitivity to the applied load.

In the second phase, a stereological technique has also been implemented on thin sections prepared from concrete disks impregnated with fluorescent dye. Digital image processing has then been carried out using fluorescent stereomicroscope to provide quantitative information on cracks geometry. The preliminary study indicates promising contribution of low-invasive methods for evaluation of damage in RC elements.

1 INTRODUCTION

Post-earthquake damage evaluation must be conducted to determine the appropriate remediation plan. This evaluation can be used in the assessment of the residual capacity of existing damaged RC buildings, allowing vulnerable structures which cannot withstand further seismic actions to be distinguished (Maeda et al. 2004). This provides authorities with a basis to make a decision, as to whether damaged structure to be demolished, repaired or even accepted without repair. To this end, reliable data collection is needed by employing well suited low-invasive techniques to characterize both constituents in a RC member; concrete material and steel rebar; separately. This study addresses the former component as a more unknown and challengeable materials due to its heterogeneity property while the supplementary work on steel part could be found somewhere else (Loporcaro et al. 2014).

Several types of non-destructive test (NDT), from the simple rebound hammer test to a highly sophisticated technique such as computational tomography (CT), have been proposed to examine the properties of concrete material. Since it is most preferable to characterize structural response by Engineering Demand Parameters (e.g. drift ratio, strain and deformation), this study was aimed to find a correlation between level of damage in the concrete and strain. As a result, finding practical techniques which are applicable during site investigation is of vital importance. Table 1 summarizes a brief review on the applicability of all available methods with regard to their advantages as well as shortcomings.

Table 1. Non Destructive Test Type Applications, Advantages and Limitations.

Type of test		Application	Advantages	Limitations
Visual tests (Perenchio 1989)		The first step to investigate concrete material	Quick evaluation of damage	No detailed information
Rebound hammer (Greene 1954)		Measuring surface hardness of concrete to estimate compressive strength	The assessment of the surface layer strength	Results can only suggest the hardness of surface layer
Pull-out (Tremper 1944)		In-place estimation of the compressive/tensile strengths	In-place strength of concrete	Pre-inserted pullout device
Pull-off/Tear-off (Long and McC 1984; Stehno and Mall 1977)		Direct tension test	In-situ tensile strength of concrete Determining bond strength between existing concrete and repair material	Sensitivity to rate of loading
Penetration probe (Windsor probe) (Arni 1972)		Estimating compressive strength, uniformity and quality of concrete. Measuring the relative rate of strength development of concrete at early ages	Determination of in situ quality of concrete. The results are not subject to surface conditions and moisture content	Minimum edge distance and member thickness slightly damages in test area
Durability test	Concrete Electrical resistivity (Malhotra 1986)	Measuring the ability of the concrete to conduct the corrosion current	Inexpensive, simple and many measurements can be made rapidly	It is not reliable at high moisture contents
	Permeability (Grube and Lawrence 1984)	To evaluate the transfer properties of concrete (porosity)	Useful method to evaluate the risk of leaching, corrosion, and freezing	Thickness limitation. Age, temperature dependent. Sufficient lateral sealing
Fiberscope (Hartbower 1996)		To check the condition of cavities, and honeycombing in reinforced concrete Voids detection along grouted post-stressed tendons	Direct visual inspection of inaccessible parts of an element	Semi destructive as the probe holes usually must be drilled. Needs for additional fibre to carry light from an external source inspected
Ground penetrating radar (Morey 1974)		Location of reinforcement Depth of cover Location of voids Location of cracks In situ density Moisture content	Survey large areas rapidly	Results must be correlated to test results on samples obtained Low level signals from targets as depth increases Expensive to use small areas
Stress-Wave propagation methods	Ultrasonic pulse velocity (Long et al. 1945)	Determination of concrete quality by measuring pulse velocity	Excellent for determining the quality and uniformity of concrete especially for rapid survey of large areas and thick members	Need for access to the other surface No information about the depth of suspected flaw
	Ultrasonic echo method (Mailer 1972)	Quality control and integrity of concrete	Access to only one face is needed. Internal discontinuities and their sizes can be estimated	Limited member thickness
	Impact echo method (Sansalone and Carino 1986)	Defects within concrete element such as delamination, voids, honeycombing	Access to only one face is needed	The ability of instrument is limited to less than 2 m thickness

	Type of test	Application	Advantages	Limitations
Nuclear methods	Spectral analysis of surface waves (Jones 1962)	Determining the stiffness profile of a pavement Depth of deteriorated concrete.	Capability of determining the elastic properties of layered systems such as pavement and interlayered concrete	Complex signal processing
	Radiography (Mullins and Pearson 1949)	Locating internal cracks, voids and variations in density of concrete	Simple to operate, and is applicable to a variety of materials	X-ray equipment is bulky and expensive. It is difficult to identify cracks perpendicular to radiation beam.
	Backscatter radiometry (Forrester 1969)	Determining in-place density of fresh or hardened concrete	Access only to surface of test object. Since this method measurements are affected by the top 40 to 100 mm, the method is best for assessing surface zone of concrete element	The accuracy of this method is lower than direct transmission. Measurements are influenced by near surface material and sensitive to chemical composition
	CT scanning (Karihaloo and Jefferson 2001)	Concrete imaging	3D crack/damage monitoring	Sophisticated software for analysis Not in-situ application Access to CT scanner Expensive technique
	Infrared Thermography (Kunz and Eales 1985)	Detecting delamination, heat loss and moisture movement through concrete elements especially for flat surfaces	No need for direct access to surface Providing an indication of the percentage of deteriorated area in survey region	Reference standards are needed Very sensitive to thermal interference from other heat sources The depth and thickness of subsurface anomaly cannot be measured
	Ultrasonic Tomography (MIRA)(Bishko et al. 2008)	It uses high frequency (greater than 20,000 Hz) sound waves to characterize the properties of materials or detect their defects	Thickness measurement, reinforcement location, and distress evaluation	Significant efforts and user expertise are required for measurement and data interpretation of large-scale application
	Acoustic Emission (Schofield 1963)	Structural health monitoring/ materials characteristics through capturing acoustical signals where an event source occurred.	Detecting the initiation and growth of cracks in concrete under stress A few transducers are enough to detect and locate defects over large areas	Passive technique; it could be used when the structure is under loading
	Petrography (Christensen et al. 1979)	Forensic investigation of concrete Determining the composition and identifying the source of the materials Determination of w/c Determining the depth of fire damage	Microscopic examination of concrete samples	Lab facilities as well as high experienced personnel is needed to interpret the result

The cracks in concrete which are indicatives of structural damage allows for a rapid fluid transport, resulting in higher permeable material (Wiwattanachang and Giao 2011). As a result, oxygen permeability tests, electrical resistivity tests and porosity tests, which are often used for durability testing, are employed to determine which is best for a certain purpose. This study intends to evaluate the level of damage occurred after an earthquake through the identification of the effect of damage incurred by axial loading on the permeability, resistivity and porosity of damaged concrete samples after unloading. A load applied up to the 90% of the ultimate strength is assumed to generate

considerable macroscopic cracking as a significant increase in permeability index has been obtained (Djerbi Tegguer et al. 2013). To achieve further information on the effect of load-induced micro cracking on the gas permeability of ordinary concrete after an earthquake, the specimens were loaded up to 50%, 70% and 95% of ultimate strength while the strains were measured. The damaged specimens were then prepared for testing in standard conditions as it will be described in the following.

2 EXPERIMENTAL PROGRAMS

2.1 Materials, Mix Proportion and Specimen Details

The ordinary concrete mix was prepared in accordance with the New Zealand Standard, NZS 3104:2003. Locally available semi-crushed coarse aggregate (maximum size 13 mm), fine aggregate (natural river sand), and drinkable water were used in concrete mix. Both aggregates were pre-soaked in water before batching so that the moisture content (3%) was above the saturated-surface dry (SSD) condition (0.9%). General Purpose cement (GP) was used. No fly ash, super plasticiser and fibre were implemented. A Water Reducing Admixtures (WRA) was added to achieve a slump of 90 ±10 mm. Table 2 presents the quantities of the mix proportions per cubic metre of concrete.

Table 2. Concrete constituents and mix proportions.

Mix proportions of concrete	
Material	OC
Coarse aggregate (kg/m^3)	1050
Fine aggregate (kg/m^3)	850
Cement (kg/m^3)	292
Water (kg/m^3)	175
Average compressive strength at 28 days (MPa)	47.6
Average compressive strength at 90 days (MPa)	71

In the mixing procedure adopted in this experiment, about two-thirds of the required water was added to the aggregates in a 150 litre capacity drum mixer before introducing cement to the mix. Cement was then added to the mix when the aggregates and water were mixed for approximately 2 min. This is followed by continuous peeling of concrete clots stick around the inside face of the drum. The remaining portion of water as well as WRA was then poured into the mixer and another minute of mixing followed.

Concrete cylinders of height 200 mm and diameter100mm, were cast in steel moulds at three layers from a single batch. Each layer was compacted using a vibrating table with mounting possibility of forms. All mixing and casting was carried out at standard laboratory conditions of 23± 2°C. After casting the cylindrical specimens were stored in a room maintained at 20°C and about 50% relative humidity (RH) for 24 h. The cylinders were then demoulded and moist-cured in 95% RH to the age of 28 and 90 days.

2.2 Mechanical Damaging

For test preparation the top surface of concrete cylinders was ground using a grinding machine. This causes a slight reduction in the original height of cylinders. A height modification factor was therefore needed to be applied to each sample during loading to estimate the relevant bearing load. The capping process plays a key role as it causes the load to be evenly distributed on loaded face. Two PL-60-11 strain gages (TML Tokyo Sokki Kenkyujo) were longitudinally attached on each cylinder to measure the axial strain. To account for any asymmetric longitudinal strain inconsistency, strain gages were mounted at every 180° intervals. The circumferential strains were also measured using the same type strain gages laid on both sides of each specimen (Fig. 1a). Three witness samples at both ages (28 days

and 90 days) were loaded using a cyber-plus compression machine of 3000 KN capacity (MATEST evolution) up to failure to determine average ultimate load bearing capacity of cylinders. The cylindrical samples were then subjected to progressive uniaxial compressive loading up to predefined load levels varying from 50% to 95% of the ultimate strength at the rate of equal to 2kN/s to experience mechanical damage. Figure 1.b illustrates the full compressive behaviour of 3 concrete cylinders in uniaxial compression up to failure obtained from the average readings from both strain gages at each sample. The partial compressive responses of specimens during the loading procedure up to 70, 90 and 95% of ultimate strength are plotted in Figure 1.c.

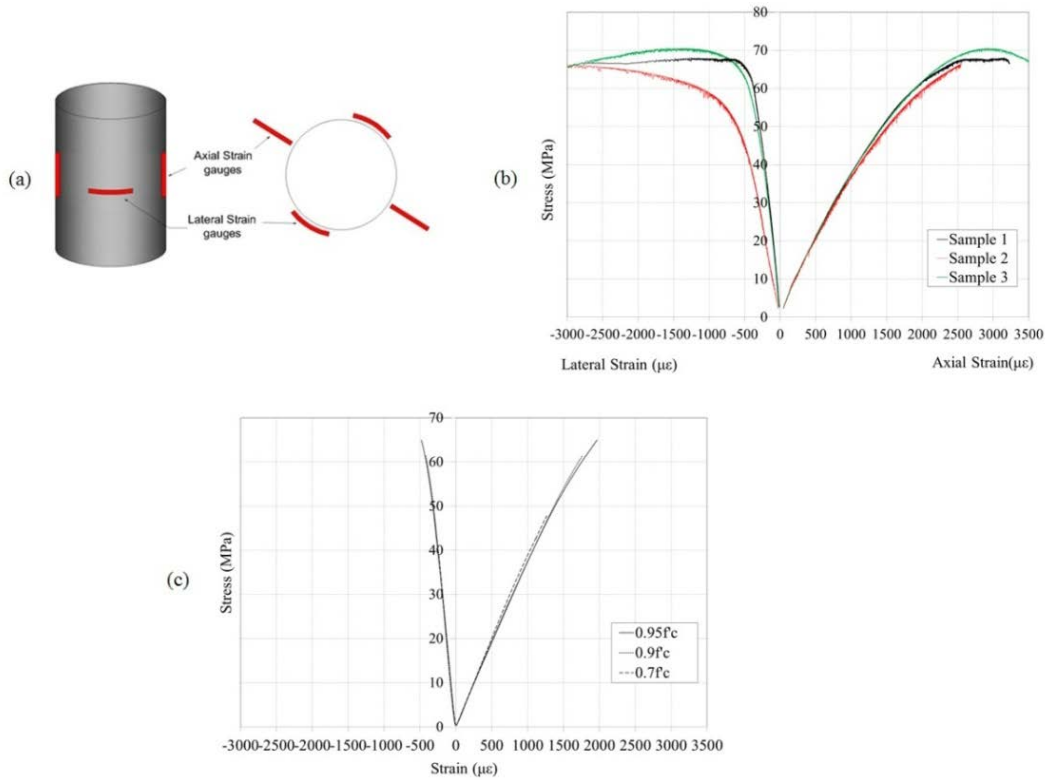

Figure 1. (a) Configuration of axial and lateral strain gauges (b) Stress-Strain relationship for plain concrete (c) Stress-strain response of cylinders corresponding to applied stress levels.

2.3 Specimen Preparation for Durability Tests

Once concrete cylinders were unloaded, damaged samples were cut using diamond blade saw at the middle one third of the height in a way that two 25mm-thick disks were extracted (Fig. 2). To eliminate any end effect, two discs were extracted from each central portion of the cylinder. Their thickness was measured with an accuracy of 0.1 mm. The discs need to be completely dried before proceeding to any gas permeability test. Figure 2.b shows the oven-dried disks at 50°C for 20 days. This temperature was found to have a minimum side effect on samples. To assure that disks are completely dried, the difference between their two consecutive mass should be less than 0.1%. Although the sample preparation process including above-mentioned steps may affect the microstructure of concrete, this additional damage was neglected in this study.

2.4 Gas Permeability Test Procedure

A permeability cell was utilised to determine the permeability index (Ballim 1991). This is a constant head permeameter test set up in which oxygen is used as the permeating substance. The cell consists of inlet and outlet valves which allow oxygen flows through the chamber. To ensure a uni-dimensional gas flow, concrete disks are sealed by a tightly silicone rubber collar fitting against the curved surface. The specimens were then placed at the top of the permeability cell, and a pressure head difference up to 100KPa was applied (Figure 3). Permeability measurements were conducted in an air-conditioned room (20 ± 1 °C and RH 50 ± 5%). After initiating the percolation of oxygen through the disks,

sufficient time (varying from 40 min to several hours) is needed to come up with steady state gas flow. The pressure decay of oxygen is recorded by transducer at 5 minute time intervals. The test is terminated either after 8 hours or a 50kPa drop in pressure.

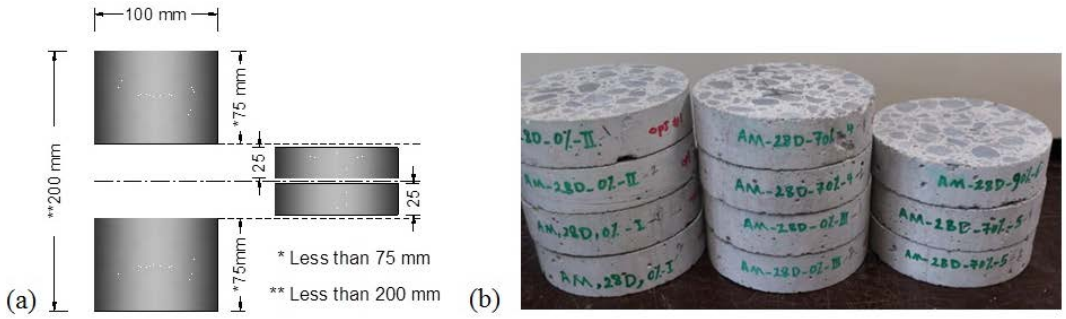

Figure 2. (a) Schematic procedure to extract concrete disks (b) Real sawn specimens.

Figure 3. Oxygen permeability test apparatus.

The apparent coefficient of permeability (m/sec) is calculated from the expression of Eq. (1) for laminar flow of a compressible fluid (Alexander et al. 1999).

$$k = \frac{\omega V g d z}{RA\theta} \quad (1)$$

Where ω is the molecular mass of oxygen (kg/mol) , V is the volume of oxygen under pressure (m^3), g is the acceleration due to gravity (m/s2), d is the sample thickness (m), z is the slope of line $\ln(P_o/P_t)$, R is the gas constant, A is the cross-sectional area (m^2), θ is the absolute temp (°k), P_o is the Initial pressure reading at the start of the test, P_t is the subsequent pressures during experiment obtained at each step.

2.5 **Electrical Resistivity Test**

Parallel plate resistivity technique in which the concrete disks are placed between two electrodes was employed in this study to measure the resistivity of concrete (Smith 2006). To conduct this experiment all concrete disks need to be completely water saturated. To allow all air bubble to be evacuated from pores, concrete disks are put in a specific chamber to experience negative pressure for 3 hours. This is followed by sucking water from supplementary water reservoir. Samples were then immersed in water for another 18 hours at which they are ready to be tested (Fig. 4a). The resistivity meter consists of two electrodes, so that one of the electrodes is attached to the negative pole of a power supply and the other one is attached to the positive (Fig. 4b). The electrical current is passed by the ions in the pore solution of the concrete – the cement matrix acts as an insulator – so it is therefore reasonable to assume that the current would follow a similar path as any ions as they move into the concrete. Resistance of concrete against electricity can then be calculated using Ohm's Law by substituting the average voltage as well as current measured across the sample. This method is cost effective and time saving, so it could be easily implemented on cylinders or cores taken from structures.

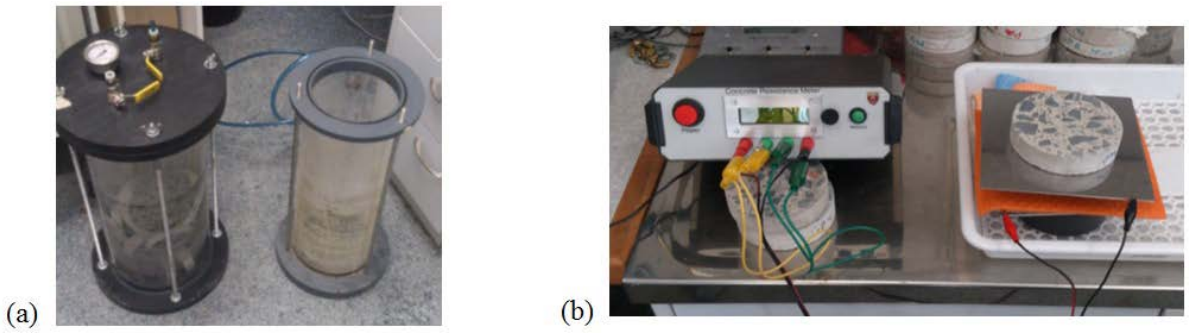

Figure 4. (a) Vacuum chambers (b) Electrical resistivity meter.

2.6 **Porosity Test**

As a further study into damaged concrete, the viability of porosity test was investigated. Two approaches were followed to evaluate the porosity of damaged concrete disks. The first experiment was carried out in accordance to conventional method described in ASTM C 642-13. In the next step the recently proposed procedure by (Montes et al. 2005) was adopted to calculate the porosity.

2.7 **Imaging Detection**

2.7.1 *Micro-CT*

Advances in computational tomography (CT) technology enable researchers to investigate crack propagation in mortar samples (Landis et al. 2003). For the purposes of this research efforts were put to use the current Micro CT machine available in the Physics lab of the University of Canterbury to examine whether it is able to capture micro-cracks in a concrete core sample extracted from damaged RC column. It was found that this machine is handicapped to reveal cracks less than 0.5mm in width in sample. As it is illustrated in Figure 5, no observable damage could be found in the cross-sectional image reconstructed from a 50 mm core taken from plastic hinge region of damaged RC column.

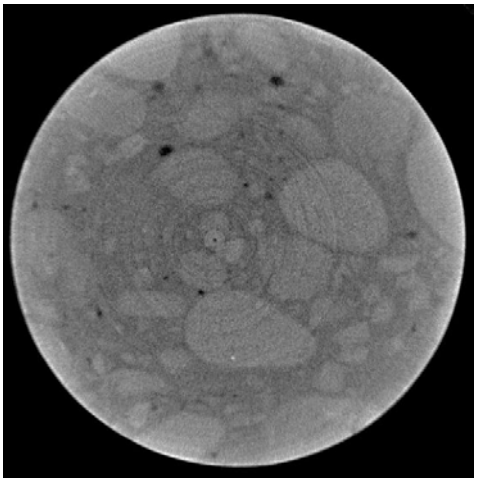

Figure 5. Reconstructed 2D view of concrete core.

2.7.2 *Microscopic Investigations*

As the outcomes of feasibility study on micro CT-scanning showed it is inapplicable, digital photomicrography investigation was used for monitoring flaws inside the concrete. In this method a magnified digital image is taken of microscope slide by utilizing a stereomicroscope to visualize internal structure of the concrete. For this purpose, completely dried disks obtained from damaged cylinders were put at a constant pressure of 100kPa in a vacuum chamber (desiccator) for 24 hours. The next day, the valve of desiccator was then opened through which the epoxy resin containing fluorescent dye sucked into the chamber. Concrete disks are then soaked in the chamber for another day to let the epoxy penetrate into the specimen and settle in cracks and other defects (Fig. 6a). The negative pressure inside the chamber is eventually released and the hardener is added to the mix to

harden impregnated dye throughout the disks. An excess of resin at the surface of the specimen was removed by grinding down 2 mm from the surface. In the next step, the vacuum-impregnated reground plane section technique proposed by (Henrichsen and Laugesen 1994) was employed to prepare more representative thin petrographic sections. These sections are basically microscopic glass slides which are attached to a thin cross-sectional slice of concrete cut from the concrete disks left from permeability test. The narrow slide of concrete is then ground smoothly using progressively fine abrasive grit until the sample is only 30 μm thick (Fig. 6b). Microscopic observation of the impregnated reground polished specimens was performed by means of a stereo Nikon Eclipse 80i microscope (see Fig. 6c) at a magnification of 10× in ultraviolet light. Figure 6d shows a microcrack of damaged concrete specimen captured in a fluorescent photomicrograph.

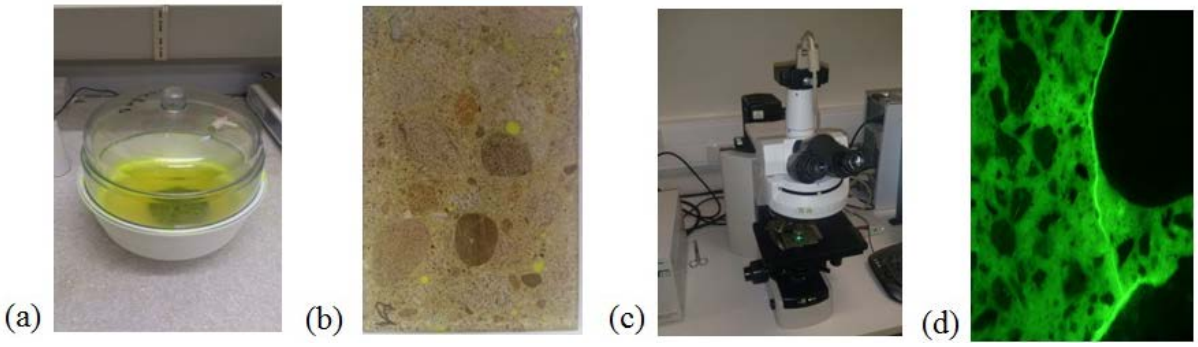

Figure 6. (a) the vacuum impregnation system (b) A thin petrographic section (c) Fluorescent microscope (d) Photomicrograph of damaged concrete specimen.

3 RESULTS AND DISCUSSION

3.1 Effect of Stress Level on Permeability

The test results plotted in Figure 7a shows as the load increases, the coefficient of permeability follows an ascending trend. This happens due to the extensive propagation of microcracks throughout the matrix connecting with other mortar cracks as well as bond cracks. Compressive load below $50\%f'_c$ does not cause any significant rise in permeability which means no considerable damage occurred in concrete material. However, the findings demonstrates at stress level varies between $50\%f'_c$ to $70\%f'_c$ the bond cracks increase in length, width and number which complies with (Picandet et al. 2009). The cracks network begins to become more interconnected at stress level of $70\%f'_c$ and beyond which forms “continuous cracks” as classified by (Shah and Chandra 1968). At $95\%f'_c$ interconnected micro cracks initialize crack formation. This is a threshold above that, a marked increase of permeability takes place.

Figure 7b indicates the variation of electrical resistivity with respect to applied stress level. In contrast to permeability coefficient, there is no significant increase in resistivity. Whilst resistivity shows a slight decrease over the whole applied stress for 28 days samples, no meaningful trend could be seen for the elder one. This implies that resistivity test is not reliable enough to be used for post-earthquake damage evaluation. The results of both porosity test methods are illustrated in Figure 7c. Although there is a trivial difference between two approaches, no interpretative change could be found over a vast range of applied stress.

3.2 Effect of Age on Permeability

This study shows that the coefficient of permeability for specimens tested at 28 days is higher than those examined at 90 days (see Fig. 7a). This demonstrates permeability decreases as concrete strength increases which confirm the existence of a correlation between the strength of concrete and transport properties of concrete proposed by (Tawfiq et al. 1996).

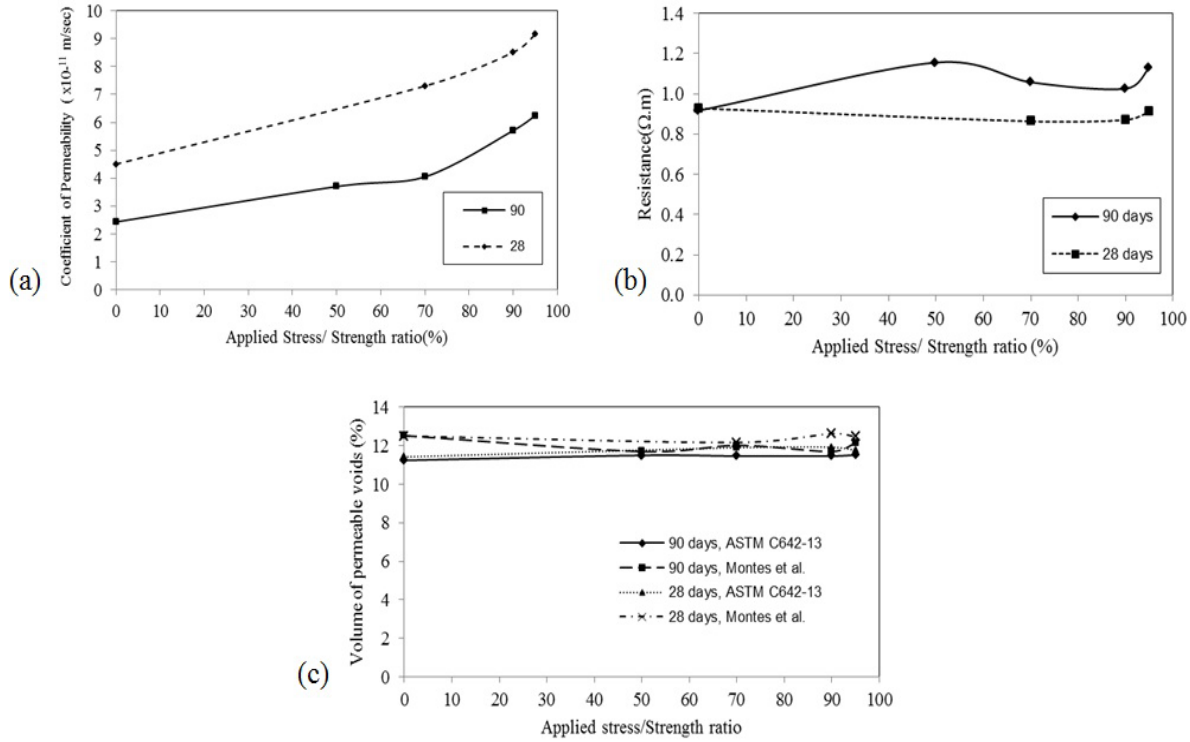

Figure 7. (a) Relationship between applied stress level and permeability coefficient (b) Relationship between applied stress level and electrical resistance (c) Relationship between applied stress level and permeability.

3.3 Assessment of Damage and Residual Strength

The residual stress-strain responses of the partially damaged concrete cylinders after exposure to predefined monotonic compressive stress levels are illustrated in Figure 8a. The compressive strength decreases continuously with an increase in compressive loading, and the increase rate is higher for the loading level above 70% ultimate strength. The residual strength after experiencing 50%f'_c still retains about the same value of the original strength; however, the residual strength at 70% and 95% of ultimate strength reduce to about 95%, 85% ultimate strength in intact samples, respectively. Results also show that the strain capacity decreases compared to original intact specimens. This could imply that damage (e.g. crushing) would occur earlier when the damaged specimen will be subjected to the next demand loading (i.e. earthquake/aftershock).

The key factor to determine remaining capacity of a damaged concrete sample is a reasonable estimation of stress level which sample has already experienced. This could be found through experimental relationship plotted in Figure 7a, when the coefficient of permeability was measured. Damage in terms of reduction in ultimate strength for monotonic loading condition can then be evaluated from Figure 8b.

3.4 Quantitative Microscopic Analysis

All the images reported in this study were acquired by a video camera attached to the microscope. Geometrical characteristics of cracks were acquired by means of Image Pro Plus 6 image analysis software on the digital images. To this end, the colorful image was converted into a binary image on the basis of its R (red), G (green) and B (blue) components through segmentation process. Figure 9 indicates a remarkable increase in the total area of microcracks; determined using image processing; when stress level increases. This could be related to the noticeable growth of cracks width and lengths once specimen undertakes more damage.

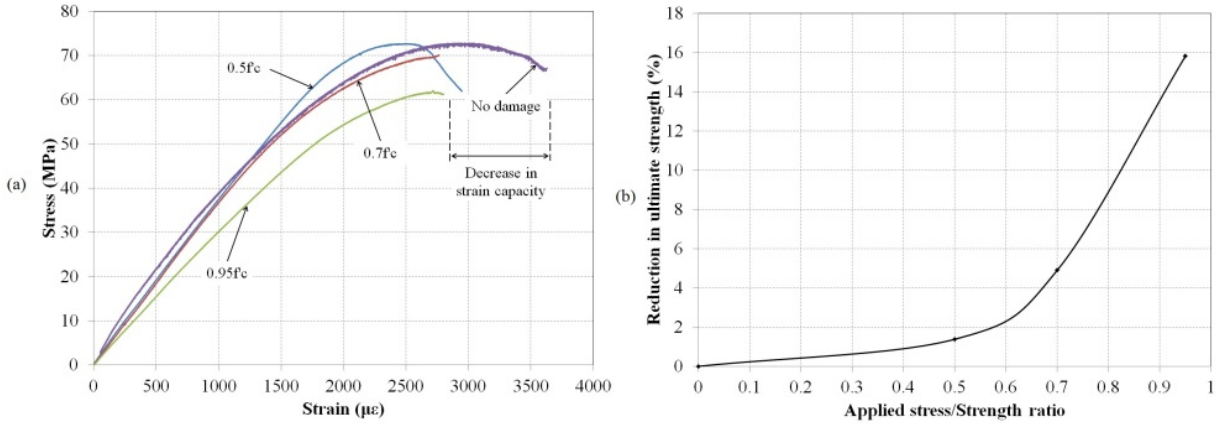

Figure 8. (a) Experimental stress-strain curves after applying different stress levels (b) The effect of damage in ultimate bearing capacity.

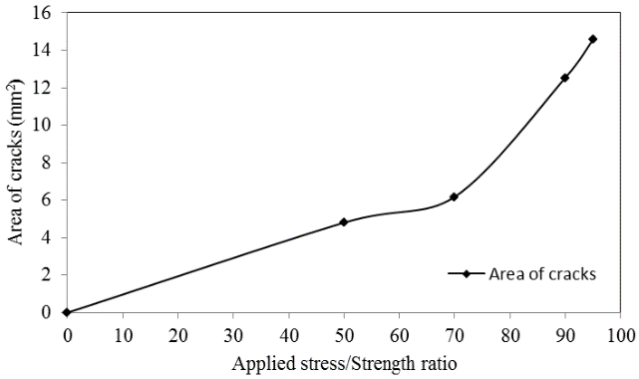

Figure 9 Variation of total cracked area during loading.

4 CONCLUSIONS

Two alternative approaches; durability tests as well as image detection; were investigated to assess the damage of concrete incurred by external uniaxial compressive loadings on cylindrical samples. In the first stage, the effect of stress on permeability, electrical resistivity and porosity of damaged samples were studied. In the next stage, microscopic imaging along with digital image processing carried out on petrographic thin section not only to capture damage qualitatively but also determine cracked areas quantitatively. Based on this work, the following conclusion can be drawn:

1. The oxygen permeability coefficient of 90 days samples increased only slightly up to the stress level of 70% of the ultimate strength. This implies that once samples get unloaded from 0.7f'c a significant amount of microcracking is recovered. For the applied stress beyond this, permeability begins to rise remarkably. A compressive load of 0.95f'c increased the permeability by about three times compared to undamaged sample due to some residual microcracks after unloading.
2. From experimental results based on monotonic testing only, it was observed that as pre-applied stress level increased, the residual strength of damaged samples decreased. This is also followed by a noticeable decrease in strain capacity.
3. Greater increase in the permeability occurred when the concrete was younger/weaker.
4. The maximum applied strain during loading directly increased the permeability index due to the formation of a connected network of microcracks. In other words, after the samples are unloaded interconnected channels did not close down completely. The effect of these irreversible cracks can be efficiently identified using permeability test.

5. In the present study, the critical stress, i.e. the point at which oxygen permeability coefficient dramatically increase for small increase in stress is found to be exceeded when the concrete cylinders were loaded to stress level between 0.7f'c and 0.95f'c.
6. Outcomes shows permeability test could be used as a useful tool to identify the level of damage in terms of permeability coefficient with respect to experienced strain/stress in damaged concrete for post-earthquake evaluation purposes.
7. In spite of a minor variation in concrete resistance, resistivity test shows no clear trend in concrete resistance over the whole range of applied stress. Results indicate that electrical resistance is not a reliable low-invasive technique to estimate the level of damage in concrete specimens.
8. Similar to resistivity test the study shows porosity test is not capable to reveal the level of damage in damaged samples.
9. The laboratory investigation revealed a good correlation between the damage represented as areas of cracks and the applied compressive stress.
10. Observation of the thin petrographic sections in ultraviolet light using a stereomicroscope at the magnification of 10 times is sufficient to detect fine cracks. The digital image processing provides a quantitative tool to determine cracks geometry.

5 ACKNOWLEDGEMENTS

The authors would like to acknowledge the funding provided for the project by the MBIE via the Natural Hazard Research Platform. Authors would also like to thank Robert Spiers, technician of the petrographic and cosmogenic laboratory at the department of geological science and also Manfred Ingerfeld, technician of the Biology lab at the department of biological science at University of Canterbury for their support throughout the experimental stage of this study.

6 REFERENCES

Alexander, M., Ballim, Y. & Mackechnie, J. 1999. Concrete durability index testing manual, Research Monograph No. 4. *Department of Civil Engineering, University of Cape Town*.

Arni, H.T. 1972. Impact and penetration tests of portland cement concrete. *Highway Research Record*(378).

Ballim, Y. 1991. A low cost falling head permeameter for measuring concrete gas permeability. *Concrete Beton*, 61: 13-18.

Bishko, A., Samokrutov, A.A. & Shevaldykin, V.G. 2008. Ultrasonic echo-pulse tomography of concrete using shear waves low-frequency phased antenna arrays. *Proc., Proceedings of the 17th World Conference on Nondestructive Testing*.

Christensen, P., Gudmundsson, H., Thaulow, N., Damgard-Jensen, A. & Chatterji, S. 1979. Structural and Ingredient Analysis of Concrete–Methods, Results, and Experience. *Nordisk Betong*, 3: 4-9.

Djerbi Tegguer, A., Bonnet, S., Khelidj, A. & Baroghel-Bouny, V. 2013. Effect of uniaxial compressive loading on gas permeability and chloride diffusion coefficient of concrete and their relationship. *Cement and Concrete Research*, 52: 131-139.

Forrester, J. 1969. Gamma radiography of concrete. *Proc., Proc. Symp. on NDT of Concrete and Timber*, 9-13.

Greene, G.W. 1954. Test hammer provides new method of evaluating hardened concrete. *Proc., ACI Journal Proceedings*, ACI.

Grube, H. & Lawrence, C. 1984. Permeability of concrete to oxygen, Cement and Concrete Association.

Hartbower, P. 1996. Fiberscope Inspection of Concrete Box Girder Bridge Sections Following the Northridge Earthquake, *Proc., Structural Materials Technology. An NDT Conference.*

Henrichsen, A. & Laugesen, P. 1994. Monitoring of concrete quality in high performance civil engineering constructions. *Proc., MRS Proceedings*, Cambridge Univ Press, 49.

Jones, R. 1962. Surface wave technique for measuring the elastic properties and thickness of roads: theoretical development. *British Journal of Applied Physics*, 13(1): 21.

Karihaloo, B., & Jefferson, A. 2001. Looking into concrete. *Magazine of Concrete Research*, 53(2): 135-147.

Kunz, J.T. & Eales, J.W. 1985. Remote sensing techniques applied to bridge deck evaluation. *ACI Special Publication*, 88.

Landis, E.N., Nagy, E.N. & Keane, D.T. 2003. Microstructure and fracture in three dimensions. *Engineering Fracture Mechanics*, 70(7): 911-925.

Long, A., & McC, A. 1984. The" Pul l-Off" Partially Destructive Test for Concrete. *ACI Special Publication*, 82.

Long, B.G., Kurtz, H.J. & Sandenaw, T.A. 1945. An Instrument and a Technique for Field Determination of the Modulus of Elasticity, and Flexural Strength, of Concrete (Pavements). *Proc., ACI Journal Proceedings*, ACI.

Loporcaro, G., Pampanin, S. & Kral, M. 2014. Investigating the relationship between hardness and plastic strain in reinforcing steel bars. *Proc., 2014 New Zealand Society of Earthquake Engineering Conference*.

Maeda, M., Nakano, Y. & Lee, K.S. 2004. Post-earthquake damage evaluation for R/C buildings based on residual seismic capacity. *Proc., 13th World Conference on Earthquake Engineering*.

Mailer, H. 1972. Pavement thickness measurement using ultrasonic techniques. *Highway Research Record*(378).

Malhotra, V. 1986. Testing Hardened Concrete: Nondestructive Methods. *ACI Monograph nº 9*, The Iowa State University Press.

Montes, F., Valavala, S. & Haselbach, L.M. 2005. A new test method for porosity measurements of Portland cement pervious concrete. *Journal of ASTM International*, 2(1): 13.

Morey, R.M. 1974. Continuous subsurface profiling by impulse radar. *Proc., Subsurface Exploration for Underground Excavation and Heavy Construction*, ASCE, 213-232.

Mullins, L. & Pearson, H. 1949. The X-Ray Examination of Concrete. *Civil Engineering and Public Works Review*, 44(515): 256-258.

Perenchio, W.F. 1989. The Condition Survey. *Concrete International*, 11(1): 59-62.

Picandet, V., Khelidj, A. & Bellegou, H. 2009. Crack effects on gas and water permeability of concretes. *Cement and Concrete Research*, 39(6): 537-547.

Sansalone, M. & Carino, N. J. 1986. Impact-echo: a method for flaw detection in concrete using transient stress waves, US Department of Commerce, National Bureau of Standards, *Center for Building Technology, Structures Division.*

Schofield, B. 1963. Acoustic emission under applied stress. Lessells and Associates Inc Waltham Ma.

Shah, S.P. & Chandra, S. 1968. Critical stress, volume change, and microcracking of concrete. *Proc., ACI Journal Proceedings*, ACI.

Smith, D. 2006. The development of a rapid test for determining the transport properties of concrete. (No. PCA R&D SN2821).

Stehno, G. & Mall, G. 1977. The tear-off method—A new way to determine the quality of concrete in structures on site. *Proc., RILEMInt. Symp. Test. In Situ Concr. Struct*, 12-15.

Tawfiq, K., Armaghani, J. & Vysyaraju, J.R. 1996. Permeability of concrete subjected to cyclic loading. *Transportation Research Record: Journal of the Transportation Research Board*, 1532(1): 51-59.

Tremper, B. 1944. The measurement of concrete strength by embedded pull-out bars. *Proc., Proc. Am. Soc. Testing Mater*, 880.

Wiwattanachang, N. & Giao, P. 2011. Monitoring crack development in fiber concrete beam by using electrical resistivity imaging. *Journal of Applied Geophysics*, 75(2): 294-304.